Experimental and numerical analysis of polarized light through random distributed spherical particles

Urachada Ketprom*, Yasuo Kuga*, Sermsak Jaruwatanadilok*, Akira Ishimaru*
Department of Electrical Engineering, University of Washington, Seattle

ABSTRACT

We have studied the polarization characteristics of light scattered from randomly distributed spherical particles using the 4x4 Mueller matrix. The experimental system consists of a Helium-Neon laser, polarizers (vertical, horizontal, 45-degree linear, left-hand circular) and six analyzers (vertical, horizontal, 45-degree linear, 135-degree linear, right-hand circular, left-hand circular). If the six polarized states of the scattered light for a given incident polarization are measured with analyzers, we can calculate the Stokes vector. By repeating this measurement for four independent incident polarizations, we can obtain the complete Mueller matrix. Random media consist of spherical particles of different concentrations suspended in water. The numerical study is based on the complete solution of the radiative transfer equation. Using the discrete ordinate method and matrix solver, we obtain the Stokes vector for a given incident polarization. By calculating Stokes vector for four independent polarizations, we can obtain a full Mueller matrix. The experimental results are compared with the numerical analysis.
Keywords: Mueller matrix, radiative transfer, polarized light, circular polarization

1. INTRODUCTION

The intensity and the polarization state of the scattered light depend on the physical parameters of the medium and the input polarization state of the incident light. To describe the complete polarimetric-characteristics of the medium, the Mueller matrix, which relates the incident Stokes vector to the scattered Stokes vector, is commonly used[2,4,5]. The Stokes vector is a 4x1 vector. Therefore, the Mueller matrix is given by a 4x4 matrix. There are several different ways to measure the Mueller matrix at microwave and optical wavelengths. If the phase of the scattered wave can be measured accurately, the scattered fields measured at two orthogonal polarizations for a given incident polarization are sufficient to provide the scattered Stokes vector[2]. This approach has been used for the millimeter-wave system. However, if the phase measurement is difficult such as in optical systems, one method to obtain the scattered Stokes vector is to measure the six different polarizations for a given incident polarization[5].

The polarization states of the scattered light from randomly distributed spherical particles have been analyzed using the Stokes vector and vector radiative transfer (RT) equation in the past[1,3,4]. Although the exact solution of the RT equation has not been obtained, the numerical solution can be obtained using different approaches including the discrete ordinate method[1,3]. This will provide the Stokes vector of the scattered intensity for a given incident polarization. Extensive numerical studies have been conducted for both linearly and circularly polarized incident waves[3]. Although detailed comparisons with experimental data have not been reported, it is believed that the RT equation will provide accurate results except for the backscattering direction in which the backscattering enhancement occurs. In this paper, we will compare the Mueller matrix calculated from the RT equation with the experimental results. The scattering medium consists of randomly distributed spherical particles suspended in water.

2. NUMERICAL METHOD TO CALCULATE THE MUELLER MATRIX

We will briefly describe the vector radiative transfer equation, numerical method, and Mueller matrix calculation. Details can be found in the references[3]. Consider the vector radiative transfer equation in a plane-parallel medium over the optical main distance domain $\tau = \rho\sigma_t Z$, where ρ is the number of density, σ_t is the total scattering cross section, and

*uketprom@ee.washington.edu,kuga@ee.washington.edu, sermsak@ee.washington.edu,ishimaru@ee.washington.edu; phone 206-543-2159; fax 206-543-3842; University of Washington, EE/CSE, Box 352500, Seattle, WA 98195 USA.

Z is the actual distance. The equation of transfer for spherical particles is then given in term of (μ,ϕ) and (μ',ϕ') where $\mu = \cos\theta$ and $\mu' = \cos\theta'$.

$$\mu\frac{d}{d\tau}[I(\tau,\mu,\phi)] = -[I(\tau,\mu,\phi)] + \int [S][I'(\tau,\mu',\phi')]d\omega' + [I_i], \tag{1}$$

$[I]$ = 4x1 incoherent specific intensity, $[Ii]$ = 4x1 incident specific intensity, $d\omega' = d\mu' d\phi'$, and $[S]$ = 4x4 scattering matrix. The scattering matrix is expressed in terms of the scattering amplitude f_{11}, f_{12}, f_{21} and f_{22}, calculated by Mie theory and explained in detail by Cheung[3].

$$[S] = \frac{1}{\rho\sigma_t}\begin{bmatrix} \rho|f_{11}|^2 & \rho|f_{12}|^2 & \rho\,\mathrm{Re}(f_{11}f_{12}^*) & -\rho\,\mathrm{Im}(f_{11}f_{12}^*) \\ \rho|f_{21}|^2 & \rho|f_{22}|^2 & \rho\,\mathrm{Re}(f_{21}f_{22}^*) & -\rho\,\mathrm{Im}(f_{21}f_{22}^*) \\ \rho 2\,\mathrm{Re}(f_{11}f_{21}^*) & \rho 2\,\mathrm{Re}(f_{12}f_{22}^*) & \rho\,\mathrm{Re}(f_{11}f_{22}^* + f_{12}f_{21}^*) & -\rho\,\mathrm{Im}(f_{11}f_{22}^* - f_{12}f_{21}^*) \\ \rho 2\,\mathrm{Im}(f_{11}f_{21}^*) & \rho 2\,\mathrm{Im}(f_{12}f_{22}^*) & \rho\,\mathrm{Im}(f_{11}f_{22}^* + f_{12}f_{21}^*) & \rho\,\mathrm{Re}(f_{11}f_{22}^* - f_{12}f_{21}^*) \end{bmatrix}. \tag{2}$$

The boundary conditions at the surface $\tau = 0$ and $\tau = \tau_o$ are obtained by noting that the diffuse intensity is generated only within the medium. Therefore, the diffuse intensity should always be pointed outward. There is no other intensity coming into the slab of random medium except the input intensity. Note that τ_o is the optical depth defined by $\tau_o = \rho\sigma_t L$ where L is length of the slab of the random medium. Mathematically, the boundary conditions are given as

$$\begin{aligned} &\text{At } \tau = 0 \quad [I] = 0 \quad for \quad 0 \le \mu \le 1 \\ &\text{At } \tau = \tau_0 \quad [I] = 0 \quad for \quad -1 \le \mu \le 0\,. \end{aligned} \tag{3}$$

The equation of transfer and its boundary conditions constitute a complete mathematical description of the problem.
The numerical solution for the above vector RT equation has been extensively studied before, and the details are discussed in the references[3]. The solution of Eq(1) is given in the form of scattered Stokes vector for a given incident polarization. To obtain the complete Mueller matrix of a random medium, we need to calculate Eq(1) for different incident polarizations. The relationship between the scattered and incident Stokes vectors is given by

$$[I_s] = \sigma[I_{io}] = \begin{vmatrix} \sigma_{11} & \sigma_{12} & \sigma_{13} & \sigma_{14} \\ \sigma_{21} & \sigma_{22} & \sigma_{23} & \sigma_{24} \\ \sigma_{31} & \sigma_{32} & \sigma_{33} & \sigma_{34} \\ \sigma_{41} & \sigma_{42} & \sigma_{43} & \sigma_{44} \end{vmatrix} [I_{io}] \tag{4}$$

where σ is the Mueller matrix, $[I_{io}]$ is the incident Stokes vector, and $[I_s]$ is the scattered Stokes vector. Eq(4) indicates that four independent $[I_{io}]$ will be required to obtain σ. One example of the Stokes vectors of four independent incident polarizations is horizontal (H), vertical (V), 45-degree linear (45), and left-hand circular (LHC) polarizations.

$$[I_{io}]^h = \begin{bmatrix} 1 \\ 0 \\ 0 \\ 0 \end{bmatrix} \qquad [I_{io}]^v = \begin{bmatrix} 0 \\ 1 \\ 0 \\ 0 \end{bmatrix} \qquad [I_{io}]^{45} = \begin{bmatrix} \frac{1}{2} \\ \frac{1}{2} \\ 1 \\ 0 \end{bmatrix} \qquad [I_{io}]^{lhc} = \begin{bmatrix} \frac{1}{2} \\ \frac{1}{2} \\ 0 \\ 1 \end{bmatrix}. \tag{5}$$

Although an ideal situation is to develop a single computer program that can handle an arbitrary incident polarization, we separate the numerical simulations into two cases in order to reduce the computational time.

2.1 Numerical solutions for a linearly polarized wave (V, H, 45) normally incident upon the medium

The numerical solutions of the linearly polarized incident wave can be obtained using the Fourier expansion in ϕ and discrete ordinate method. We express the incoherent specific intensity using the Fourier series expansion as:

$$[I] = \sum_{m=0}^{\infty} [I]_m^a \cos m\phi + \sum_{m=1}^{\infty} [I]_m^a \sin m\phi. \tag{6}$$

Because all Fourier components are decoupled and only m=0 and m=2 are required for the normal incidence, the radiative transfer equations for m=0 and m=2 are given by

Mode 0 (m = 0)

$$\mu \frac{d}{d\tau}[I(\tau,\mu,\phi)]_0 = -[I(\tau,\mu,\phi)]_0 + \int_{-1}^{1} [L]_0 [I'(\tau,\mu',\phi')]_0 \, d\mu' + [F]_0 \exp(-\tau) \tag{7}$$

where

$$[I]_0 = \begin{bmatrix} I_{01} \\ I_{02} \end{bmatrix}, \qquad [L]_0 = [S_1]_0^a, \qquad [F]_0 = \frac{1}{2}\begin{bmatrix} F_{01} \\ F_{02} \end{bmatrix}.$$

Mode 2 (m =2),

$$\mu \frac{d}{d\tau}[I(\tau,\mu,\phi)]_2 = -[I(\tau,\mu,\phi)]_2 + \int_{-1}^{1} [L]_2 [I'(\tau,\mu',\phi')]_2 \, d\mu' + [F]_2 \exp(-\tau) \tag{8}$$

where

$$[I]_2 = \begin{bmatrix} I_{1a} \\ I_{2a} \\ U_b \\ V_b \end{bmatrix}, \qquad [L]_2 = \begin{bmatrix} [S_1]_2^a & [S_2]_2^b \\ [S_3]_2^b & [S_4]_2^a \end{bmatrix}, \qquad [F]_2 = \begin{bmatrix} \frac{1}{2}F_{01} \\ -\frac{1}{2}F_{02} \\ -\mathrm{Re}(F_{03}) \\ -\mathrm{Im}(F_{03}) \end{bmatrix}.$$

The detailed derivation and descriptions are given in the references[3]. The radiative transfer equations, Eq(7) and Eq(8), are integro-differential equations in μ and μ´ which can be solved using the discrete ordinate method[1]. All variables are evaluated at discrete values of μ and μ´ between +1 and -1. The resulting form is a matrix equation that can be solved using the eigen-value and eigen-vector method. Once the specific intensity of each mode is obtained, the total incoherent specific intensity is calculated. Because different incident polarizations result in different odd and even function pairs of source Fourier expansion, therefore, the incoherent specific intensity is calculated as shown in Eq.(9a) for vertical polarization and horizontal polarization and in Eq.(9b) for 45-degree incident polarization.

$$[I]_{v,h} = \begin{bmatrix} I_1 \\ I_2 \\ U \\ V \end{bmatrix} = \begin{bmatrix} I_{01} \\ I_{02} \\ 0 \\ 0 \end{bmatrix} + \begin{bmatrix} I_{1a}\cos 2\phi \\ I_{2a}\cos 2\phi \\ U_b \sin 2\phi \\ V_b \sin 2\phi \end{bmatrix} \tag{9a}$$

$$[I]_{45} = \begin{bmatrix} I_1 \\ I_2 \\ U \\ V \end{bmatrix} = \begin{bmatrix} I_{01} \\ I_{02} \\ 0 \\ 0 \end{bmatrix} + \begin{bmatrix} I_{1a}\sin 2\phi \\ I_{2a}\sin 2\phi \\ U_b \cos 2\phi \\ V_b \cos 2\phi \end{bmatrix} \tag{9b}$$

2.2 Circularly polarized (LHC) wave normally incident upon the medium

The radiative transfer equation for the circularly polarized incident wave for a normal incidence does not have ϕ dependence[3]. In this case, there is no coupling between [I_1, I_2] and [U,V], and therefore, we can separate the equation of transfer into the following two equations

$$\mu \frac{d}{d\tau}[I]_c = -[I]_c + \int_{-1}^{1} [S_1]_0^a [I']_c \, d\mu' + [F]_0 \exp(-\tau) \tag{10}$$

$$\mu \frac{d}{d\tau}[U]_c = -[U]_c + \int_{-1}^{1} [S_4]_0^a [U']_c \, d\mu' + [F]_u \exp(-\tau) \tag{11}$$

where

$$[I]_c = \begin{bmatrix} I_1 \\ I_2 \end{bmatrix}, \qquad [U]_c = \begin{bmatrix} U \\ V \end{bmatrix}, \qquad [F]_0 = \frac{1}{2}\begin{bmatrix} F_{01} \\ F_{02} \end{bmatrix}, \quad [F]_u = \begin{bmatrix} \pm \mathrm{Im}(F_{03}) \\ \mp \mathrm{Re}(F_{03}) \end{bmatrix}.$$

These two equations can be solved separately to obtain the scattered Stokes vector. The advantages of this approach rather than dealing with a single equation are a memory size and computational time. Compared to the linearly polarized case, the numerical solutions for the circularly polarized incident wave can be obtained very quickly. The left-hand and right-hand circularly polarized intensity is given by

$$I_{rhc} = \frac{1}{2}(I_1 + I_2 - V) \tag{12a}$$

$$I_{lhc} = \frac{1}{2}(I_1 + I_2 + V). \tag{12b}$$

2.3 Transferring axis of Stokes vector

In the preceding section, the Stokes vectors are defined in terms of the vertical ($E_1 = E_\theta$) and the horizontal ($E_2 = E_\phi$) components. In practice, however, the receiver often accepts the polarization parallel to (E_x) or perpendicular to (E_y), the polarization of the incident wave. Thus, we need to obtain the Stokes vector for E_x and E_y which are linearly related to the Stokes vector for (E_1) and (E_2) in the following manner:

$$\begin{bmatrix} I_x \\ I_y \\ U_{xy} \\ V_{xy} \end{bmatrix} = \begin{bmatrix} \langle E_x E_x^* \rangle \\ \langle E_y E_y^* \rangle \\ 2\langle \mathrm{Re}(E_x E_y^*) \rangle \\ 2\langle \mathrm{Im}(E_x E_y^*) \rangle \end{bmatrix} = \begin{bmatrix} \cos^2\theta\cos^2\phi & \sin^2\phi & -\frac{1}{2}\sin 2\phi\cos\theta & 0 \\ \cos^2\theta\sin^2\phi & \cos^2\phi & -\frac{1}{2}\sin 2\phi\cos\theta & 0 \\ \cos^2\theta\sin 2\phi & -\sin 2\phi & \cos 2\phi\cos\theta & 0 \\ 0 & 0 & 0 & \cos\theta \end{bmatrix} \begin{bmatrix} I_1 \\ I_2 \\ U \\ V \end{bmatrix} \tag{13}$$

The specific intensity I_x and I_y may be called the co-polarized and cross-polarized incoherent specific intensity, respectively. For comparison with the numerical calculation, an experiment which measures [I_x I_y U_{xy} V_{xy}] is used.

3. EXPERIMENTATION

An optical system is constructed to measure the intensity and the polarization state of the scattered light using four polarizers for incident light and six analyzers for scattered light. The system consists of a Helium-Neon laser as a light source (λ = 632.8 nm), 4-position polarizers, beam expander to obtain a 20mm uniform illumination, scattering cell, 6-position analyzers, and a narrow FOV detector. A large beam size is needed to simulate a plane wave that is used in the RT equation. The system measures the intensity of the six independent polarization states of the scattered light for each of the four incident polarization states. The four incident polarization states chosen are vertical (V), horizontal (H), 45

degree (45) and left-hand circular (LHC). In addition to these four states, right-hand circular (RHC) and 135 degree (135) are added to the analyzer to measure six polarization states. The polarization of the incident laser is selected by using the λ/2 and λ/4 wave plates oriented at different angles. The accuracy of the cross-polarization measurement is usually limited by the quality of the polarizers and analyzers. In our system, the cross-pol isolation is approximately 20 dB for linear polarization and 15 dB for the circular polarization. The scattering cell, which has a dimension of 50mm diameter and 20mm path-length, is placed in front of the narrow FOV detector. The detector consists of 6-polarization state analyzers, a focusing lens and multimode optical fiber that are connected to a photo-diode. Computer-controlled stepping motors control both polarizers and analyzers. The scattering medium consists of Dow Chemical micro-particles suspended in water. The particle average size is 2.02μm, the standard deviation is 0.0135μm, and the index of refraction is n=1.588. The optical depth is controlled by changing the fractional volume of particles. We used six different optical depths τ= 0.9, 1.8, 3.6, 7.2, 14.4, and 28.8 in the experiment.

3.1 Stokes vector derivation from experimental results

The experimental system measures the relative intensity received at V, H, 45, 135, LHC and RHC polarizations for each of the four incident polarizations, V, H, 45 and LHC. Let $W_{h,}$ $W_{v,}$ $W_{45,}$ $W_{135,}$ W_{lhc} and W_{rhc} be the relative scattered intensities at the V, H, 45, 135, LHC and RHC polarization states. W_i can be defined as

$$W_h = \left\langle \left| E_x^{\,2} \right| \right\rangle \quad (14) \qquad W_v = \left\langle \left| E_y^{\,2} \right| \right\rangle \quad (15)$$

$$W_{45} = \frac{\left\langle |E_x|^2 \right\rangle}{2} + \frac{\left\langle |E_y|^2 \right\rangle}{2} + U \quad (16) \qquad W_{135} = \frac{\left\langle |E_x|^2 \right\rangle}{2} + \frac{\left\langle |E_y|^2 \right\rangle}{2} - U \quad (17)$$

$$W_{lhc} = \frac{\left\langle |E_x|^2 \right\rangle}{2} + \frac{\left\langle |E_y|^2 \right\rangle}{2} + V \quad (18) \qquad W_{rhc} = \frac{\left\langle |E_x|^2 \right\rangle}{2} + \frac{\left\langle |E_y|^2 \right\rangle}{2} - V \quad (19)$$

The total scattered intensity is the sum of the measured scattered intensities in the two orthogonal polarization states. Dividing each component by the total scattered intensity P_0, we can obtain the normalized Stokes vector. Because of a slight difference of transmission characteristics of polarizers, the total intensity measured by two polarizers having different orthogonal states of polarization may not be the same. Therefore, to normalize I_{xs} and I_{ys}, $P_0 = W_h + W_v$ is used; to normalize U_{xys}, $P_0 = W_{45} + W_{135}$ is used; and to normalize V_{xys}, $P_0 = W_{lhc} + W_{rhc}$ is used, respectively. Hence, the final normalized Stokes vectors are given by

$$\begin{bmatrix} I_{xs} \\ I_{ys} \\ U_{xys} \\ V_{xys} \end{bmatrix} = \begin{bmatrix} \dfrac{W_h}{W_h + W_v} \\ \dfrac{W_v}{W_h + W_v} \\ \dfrac{W_{45} - W_{135}}{W_{45} + W_{135}} \\ \dfrac{W_{lhc} - W_{rhc}}{W_{lhc} + W_{rhc}} \end{bmatrix}. \quad (20)$$

3.2 Mueller matrix derivation from Stokes vector

As we discussed in the previous section, the scattered Stokes vectors are related to the incident Stokes vectors by $[I_s]=\sigma[I_{io}]$ where $[I_{io}]$ is the normalized incident Stokes vector given in Eq(5), $[I_s]$ is the scattered normalized Stokes vector which is being measured experimentally and σ is the normalized Mueller matrix which can be obtained from four independent incident polarization states as shown below.

$$\begin{bmatrix}\sigma_{11}\\ \sigma_{21}\\ \sigma_{31}\\ \sigma_{41}\end{bmatrix}=\begin{bmatrix}I_{1s}^{h}\\ I_{2s}^{h}\\ U_{s}^{h}\\ V_{s}^{h}\end{bmatrix} \tag{21}$$

$$\begin{bmatrix}\sigma_{12}\\ \sigma_{22}\\ \sigma_{32}\\ \sigma_{42}\end{bmatrix}=\begin{bmatrix}I_{1s}^{v}\\ I_{2s}^{v}\\ U_{s}^{v}\\ V_{s}^{v}\end{bmatrix} \tag{22}$$

$$\begin{bmatrix}\sigma_{13}\\ \sigma_{23}\\ \sigma_{33}\\ \sigma_{43}\end{bmatrix}=\begin{bmatrix}I_{1s}^{45}\\ I_{2s}^{45}\\ U_{s}^{45}\\ V_{s}^{45}\end{bmatrix}-\begin{bmatrix}\frac{\sigma_{11}}{2}+\frac{\sigma_{12}}{2}\\ \frac{\sigma_{21}}{2}+\frac{\sigma_{22}}{2}\\ \frac{\sigma_{31}}{2}+\frac{\sigma_{32}}{2}\\ \frac{\sigma_{41}}{2}+\frac{\sigma_{42}}{2}\end{bmatrix} \tag{23}$$

$$\begin{bmatrix}\sigma_{14}\\ \sigma_{24}\\ \sigma_{34}\\ \sigma_{44}\end{bmatrix}=\begin{bmatrix}I_{1s}^{lhc}\\ I_{2s}^{lhc}\\ U_{s}^{lhc}\\ V_{s}^{lhc}\end{bmatrix}-\begin{bmatrix}\frac{\sigma_{11}}{2}+\frac{\sigma_{12}}{2}\\ \frac{\sigma_{21}}{2}+\frac{\sigma_{22}}{2}\\ \frac{\sigma_{31}}{2}+\frac{\sigma_{32}}{2}\\ \frac{\sigma_{41}}{2}+\frac{\sigma_{42}}{2}\end{bmatrix} \tag{24}$$

Although the above process is discussed in terms of processing experimental results, the same technique is applied to calculate the Mueller matrix from the numerical calculation.

4. RESULTS

The necessary input parameters to calculate the specific intensity for a given optical depth (τ) are wavelength (632.8nm), particle size (average diameter=2.02μm), particle index of refraction (n=1.588+0.0001588i), and index of refraction of the background (water, n=1.33). Equations (7,8,10,11) are solved using the discrete ordinate method with the Gauss-quadrature order = 40 for a given polarization. The incident light is normal to the surface and only two Fourier components (m = 0 and 2) are required in our calculation. The transmitted specific intensity is calculated for the optical depth of τ= 0.9, 1.8, 3.6, 7.2, 14.4 and 28.8. Equations (7,8,10,11) are only for the diffuse intensity. To calculate the total intensity, the reduced incident intensity which is given by exp (-τ), must be added in the forward direction. However, the reduced incident intensity is not important for off-axial experiment ($\theta \neq 0$) and/or for large optical depth. Therefore, the numerical simulation is shown only for the diffused received power that is given by incoherent intensity and the receiver characteristics.

$$P_{total} = \left(\pi\theta_d{}^2\right) I_d \tag{25}$$

where θ_d is the detector's half-angle field of view (FOV) in radian.

The measured FOV is 0.0035 radian, which is close to the expected FOV (0.0031 radian) based on the lens focal length and the diameter of the optical fiber. The results of transmitted power as a function of optical depth for numerical study and experiment are shown in Figure 2. As we discussed in the previous section, because of the limited isolation of polarizers and analyzers, the maximum difference between the measured co- and cross-polarization is approximately 18 dB. The large difference, which is expected from the numerical simulations for small τ, cannot be measured with our current experimental system. The noise floor of the detector is approximately -97dB which is at least 10 dB less than the lowest measured intensity. Therefore, the measured cross-pol data for large τ, which is approximately –5 to –10 dB less than the co-pol, should be an accurate measurement.

Figures 2-a to 2-e show both measured and calculated power as a function of τ at different scattering angles. The numerical calculation is performed at 40 angular positions between θ=0 and 180 degrees. Rather than using the interpolation technique, the closest to the experimental angle is shown in each Figure. The reduced coherent intensity is not included in the numerical simulations shown in Figure 2-a. At large τ, we expected the agreement between numerical simulations and experiments should be reasonably good. However, we observed that the numerical results are almost 10 dB higher than that of experimental data in all cases. This can be explained if the FOV of the detector is 1/3 of what we measured (see Eq. 25). Another possibility is the accuracy of the plane wave illumination. The laser beam is

expanded to a 10mm diameter to simulate the plane wave. Although we carefully adjusted the lens position, the small angular spread is difficult to control. We are still investigating the source of a 10 dB discrepancy. As reported previously, the different between co-pol and cross-pol of circular polarization cases is larger than that of the linear polarization cases in numerical simulations when τ is greater than 5. Although we can confirm a similar trend in our experimental results, the difference is much smaller than the numerical simulations. In most cases, the cross-pol of circular polarization incidence is not much different from that of linear polarization incidence. This may be the limitation of our polarizers and analyzers, but the difference is much smaller than the isolation of these devices. The experiment is conducted using micro-spheres suspended in water, and the detector is located outside the scattering cell (in free space). On the other hand, the numerical simulations assume that the background, which includes the observation point, is water and there is no boundary. Obviously, the polarization state of the scattered light changes as it transmits through water-glass-air boundaries. Our numerical simulation does not include these boundaries.

For the Mueller matrix, there is the same problem of equipment limitation to differentiate between the co- and cross-polarization at 18 dB or higher. Refer to Figure 3, the experimental result for the forward direction θ = 8.51 degrees and small optical depth τ = 0.9, the cross polarization, row =1 and column =1 of Mueller matrix, is 0.0193 when the true value should be close to 0.0002 as expected from the numerical study at the forward direction θ = 8.329 degrees. For higher optical depth, the cross-polarization is higher; therefore, the ratio between co-polarization, row = 2,column = 1 of Mueller matrix, to the cross polarization, row =1 and column =1 of Mueller matrix, is less. This is true for both the numerical study and experiment. The Mueller matrix from the experiment becomes closer to the numerical at higher optical depth as the result shows that at τ = 28.8 the ratio is almost the same.

5. CONCLUSIONS

This paper presents a method to obtain the Stokes vector from an experiment and compare the result to solution of the radiative transfer equation in a numerical study. Unlike the numerical simulations in which an ideal condition can be used, the experiments must be conducted with available equipment with many limitations. The major limitation in this experiment is a limited isolation of polarizers and analyzers. The comparison can be performed only when the difference between co- and cross-pol powers becomes less than 10 dB, which occurs at τ greater than 15 in most cases. With this given condition, the different between co-pol and cross-pol of circular polarization cases is larger than that of the linear polarization cases in numerical simulations, but this result is not seen clearly in the experiment. Although the trends of the measured and numerical results are similar, we have not identified the source of a 10 dB difference in total power. We also need to point out that the validity of the radiative transfer equation has not been fully verified experimentally.

ACKNOWLEDGMENT

This work is supported by the National Science Foundation (ECS-9908849).

REFERENCES

1. A. Ishimaru, *Wave Propagation and Scattering in Random Media*, 574 pages, IEEE Press, Piscataway, New Jersey and Oxford University Press, Oxford, England, an IEEE-OUP Classic Reissue, 1997.
2. F. Ulaby and C. Elachi, *Radar Polarimetry for Geoscience Applications*, Artech House, 1990.
3. R.L. Cheung, and A. Ishimaru, "Transmission, Backscattering, and Depolarization of Waves in Randomly Distributed Spherical Particles," *Applied Optics*, **21**, pp. 3792-3798, 1982.
4. Q. Ma, A. Ishimaru, P. Phu, and Y. Kuga, "Transmission, reflection, and depolarization of an optical wave for a single leaf," *IEEE Transactions on Geoscience and Remote Sensing*, **28**, pp. 865-872, September 1990.
5. P. Phu, *Optical Mueller Matrix Measurement System*, M.S. thesis, University of Washington, Seattle, Washington, 1989.

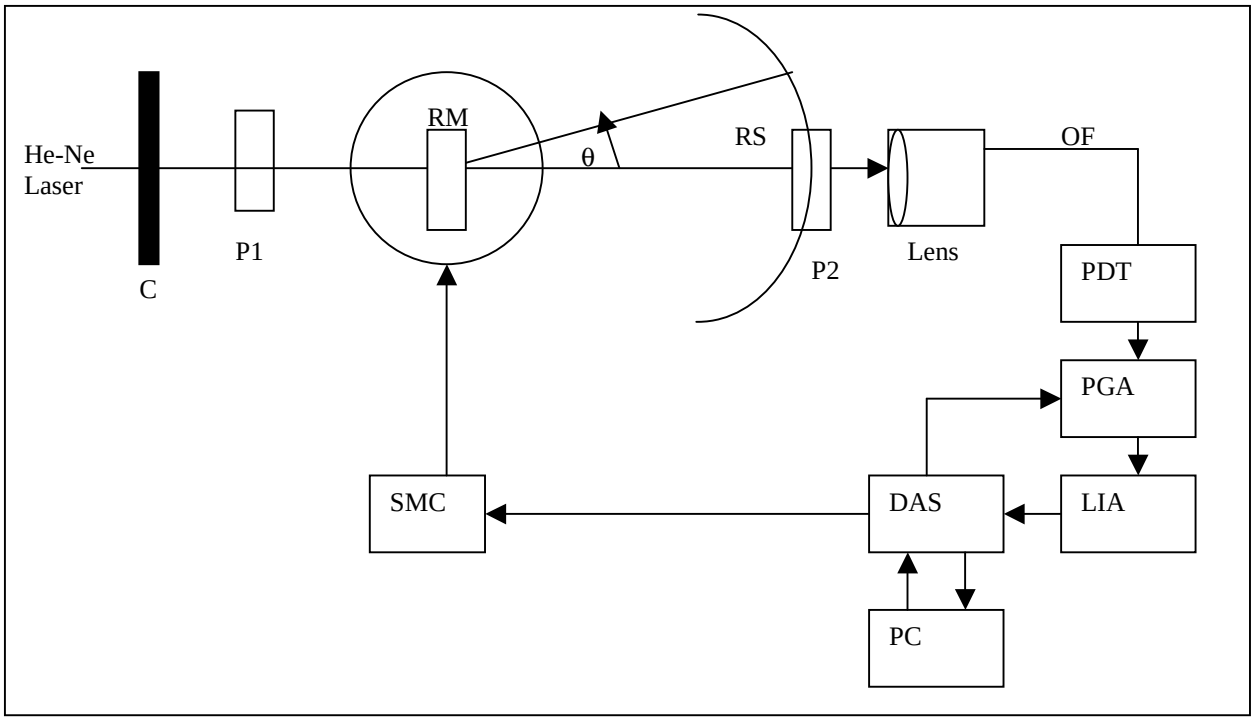

C = Chopper P1= Polarizer P2 = Analyzer OF = Optical Fiber RM = Random Media RS = Rotational Stage
PDT = Photo detector PGA = Programmable Gain Attenuator LIA = Lock-In-Amplifier
DAS = Data acquisition system PC = IBM Personal Computer SMC = Stepping motor controller

Figure 1: Setup Diagram

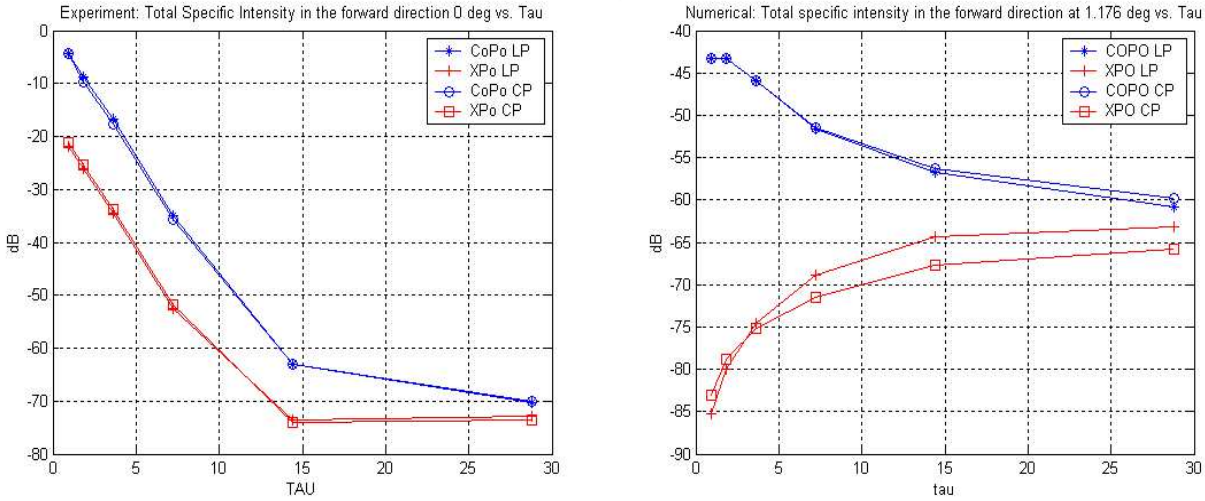

Figure 2-a: Experiment: θ_s=0 degrees, numerical θ_s=1.176 degrees.

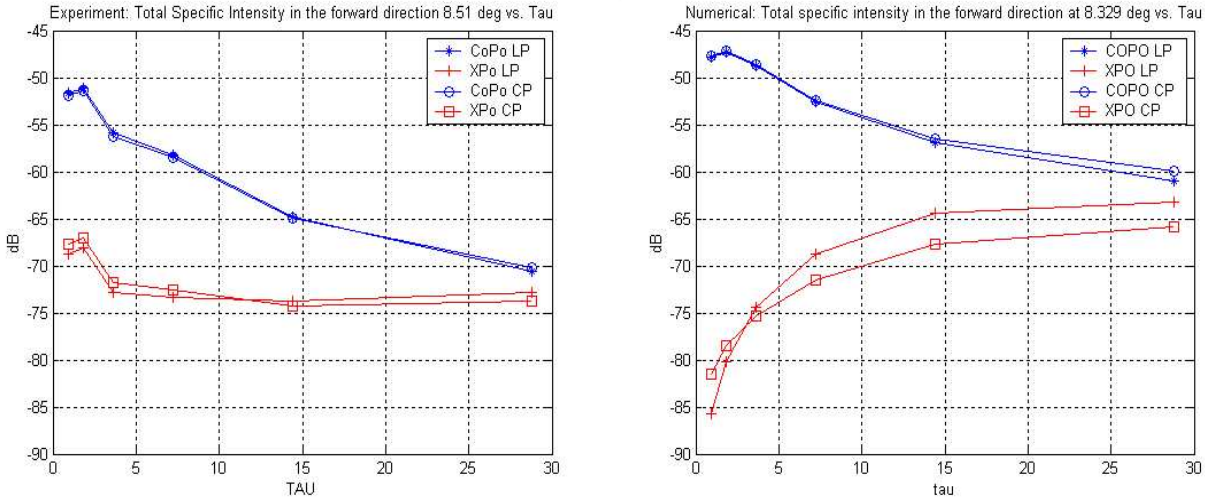

Figure 2-b: Experiment: θ_s=8.51 degrees, numerical θ_s=8.33 degrees.

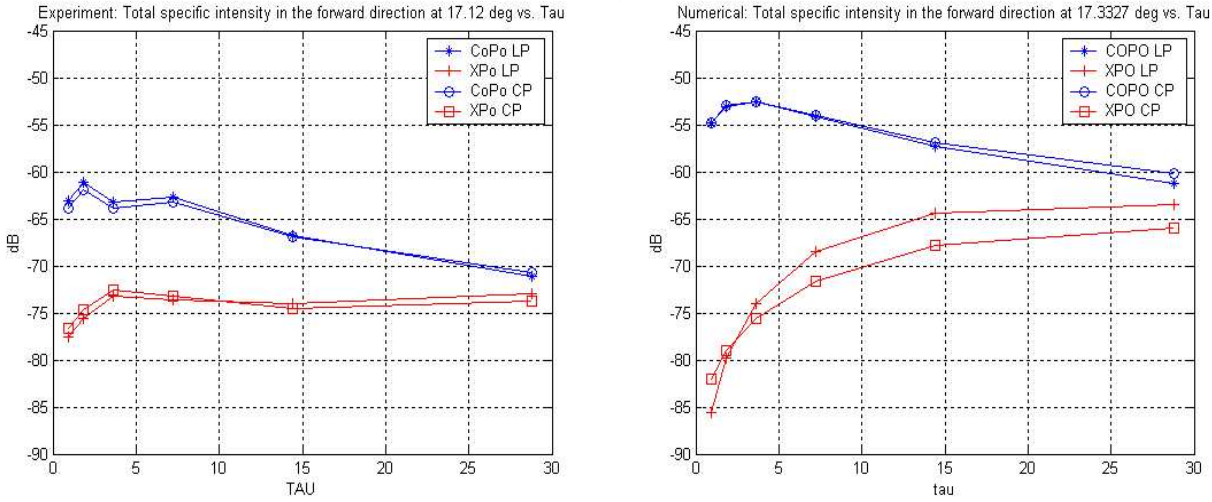

Figure 2-c: Experiment: θ_s=17.12 degrees, numerical θ_s=17.33 degrees.

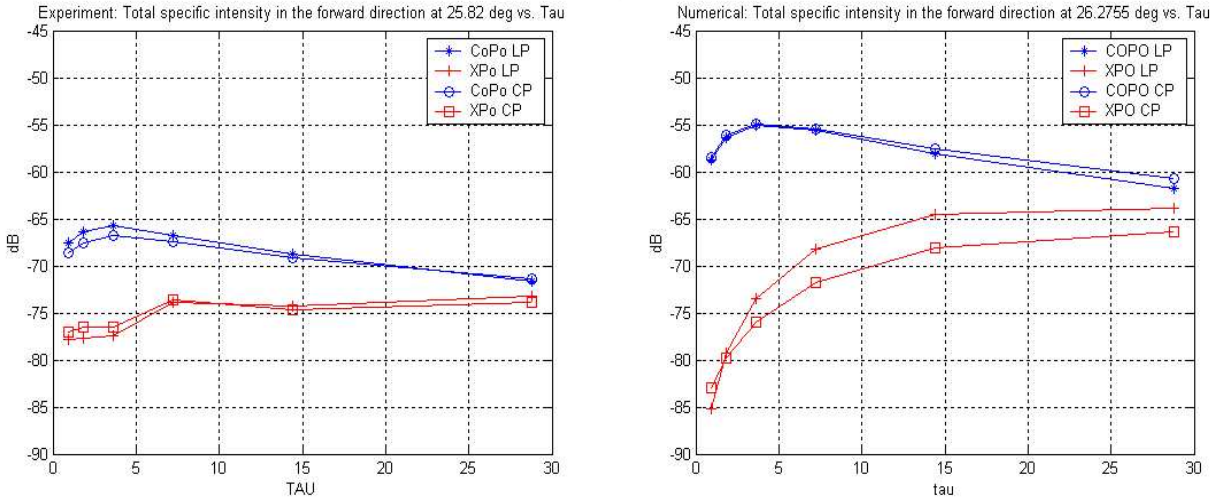

Figure 2-d: Experiment: θ_s=25.82 degrees, numerical θ_s=26.27 degrees.

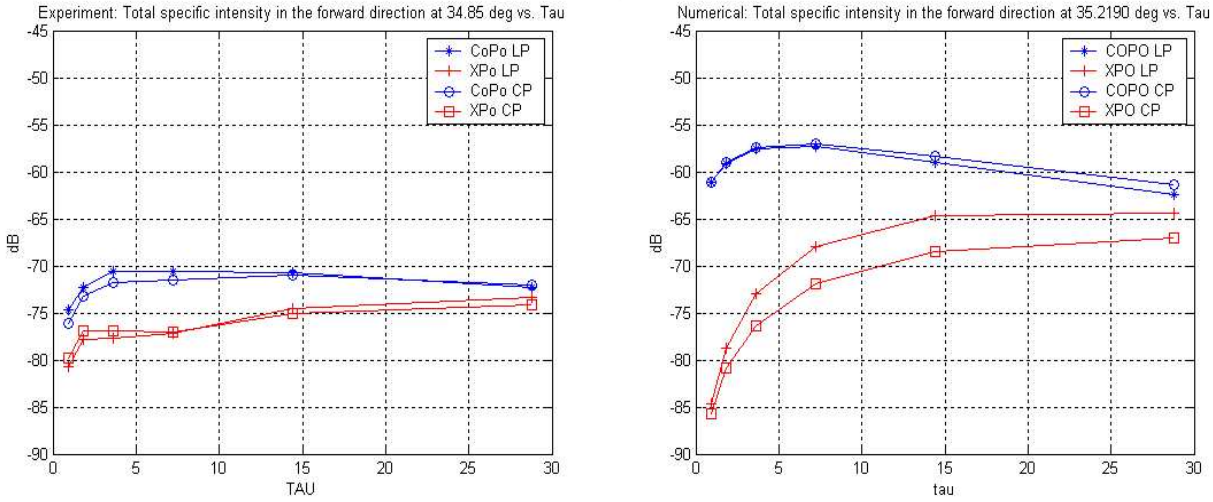

Figure 2-e: Experiment: θ_s=34.84 degrees, numerical θ_s=35.22 degrees.

Normalized Mueller matrix from experiment Deg = 8.51	**Normalized Mueller matrix from numerical Deg = 8.3926**
tau = 0.9000 deg = 8.51 0.0193 0.9880 -0.0536 0.0456 1.0000 0.0313 0.0536 -0.0456 0.0249 0.1636 -1.0574 -0.0661 0.1051 -0.0205 0.0146 0.9254	tau = 0.9000 theta = 8.3926 0.0002 1.0382 0.0000 0.0000 1.0000 0.0002 -0.0000 0.0000 0 0 -1.0186 0.0183 0 0 0.0183 1.0184
tau = 1.8000 deg = 8.51 0.0196 0.9878 -0.0456 0.0421 1.0000 0.0318 0.0456 -0.0421 0.0330 0.1646 -1.0597 -0.0735 0.1256 -0.0428 0.0101 0.9241	tau = 1.8000 theta = 8.3926 0.0005 1.0333 0.0000 0 1.0000 0.0005 -0.0000 0 0 0 -1.0158 0.0143 0 0 0.0143 1.0156
tau = 3.6000 deg = 8.51 0.0200 0.9869 -0.0479 0.0359 1.0000 0.0331 0.0479 -0.0359 0.0329 0.1671 -1.0610 -0.0117 0.1055 -0.0328 0.0319 0.9277	tau = 3.6000 theta = 8.3926 0.0027 1.0234 0.0000 0.0000 1.0000 0.0027 -0.0000 0 0 0 -1.0088 0.0078 0 0 0.0078 1.0099
tau = 7.2000 deg = 8.51 0.0312 0.9855 -0.0411 0.0542 1.0000 0.0457 0.0411 -0.0542 0.0309 0.1648 -1.0470 -0.0551 0.1195 -0.0435 0.0030 0.9149	tau = 7.2000 theta = 8.3926 0.0240 1.0087 0.0000 0.0000 1.0000 0.0240 -0.0000 0 0 0 -0.9803 0.0012 0 0 0.0012 1.0030
tau = 14.4000 deg = 8.51 0.1269 0.9811 -0.0325 -0.0071 1.0000 0.1458 0.0325 0.0071 0.0449 0.1444 -0.9556 -0.0775 0.0928 0.0136 -0.0095 0.8443	tau = 14.4000 theta = 8.3926 0.1779 1.0011 0 0 1.0000 0.1779 0 0 0 0 -0.8226 0.0004 0 0 -0.0005 1.0144
tau = 28.8000 deg = 8.51 0.5925 0.9687 0.0068 0.0218 1.0000 0.6238 -0.0068 -0.0218 0.0413 0.0685 -0.4568 -0.0191 0.0723 0.0264 -0.0599 0.5497	tau = 28.8000 theta = 8.3926 0.5855 1.0001 0 0 1.0000 0.5856 0 0 0 0 -0.4145 0.0002 0 0 -0.0003 0.9361

Normalized Mueller matrix from experiment Deg = 25.82	**Normalized Mueller matrix from numerical Deg = 26.2775**
tau = 0.9000 deg = 25.82 0.0916 0.9416 -0.0621 0.0220 1.0000 0.1500 0.0621 -0.0220 0.0179 0.1475 -0.9201 -0.0454 0.1105 -0.0207 0.0067 0.7735	tau = 0.9000 theta = 26.2755 0.0023 1.1312 0.0000 0 1.0000 0.0022 -0.0000 -0.0000 0 0 -1.0591 0.0237 0 0 0.0238 1.0603
tau = 1.8000 deg = 25.82 0.0741 0.9418 -0.0595 0.0178 1.0000 0.1323 0.0595 -0.0178 0.0245 0.1506 -0.9565 -0.0411 0.0897 -0.0066 0.0081 0.7930	tau = 1.8000 theta = 26.2755 0.0051 1.0895 0.0000 0.0000 1.0000 0.0050 -0.0000 0 0 0 -1.0370 0.0075 0 0 0.0076 1.0408
tau = 3.6000 deg = 25.82 0.0690 0.9502 -0.0669 0.0036 1.0000 0.1188 0.0669 -0.0036 0.0354 0.1546 -0.9726 -0.0072 0.0962 0.0042 -0.0059 0.8160	tau = 3.6000 theta = 26.2755 0.0145 1.0537 0.0000 -0.0000 1.0000 0.0143 -0.0000 0 0 0 -1.0111 0.0035 0 0 -0.0033 1.0250
tau = 7.2000 deg = 25.82 0.1953 0.9230 -0.0189 0.0350 1.0000 0.2723 0.0189 -0.0350 0.0426 0.1089 -0.7614 -0.0413 0.0884 -0.0100 -0.0157 0.6869	tau = 7.2000 theta = 26.2755 0.0559 1.0263 0.0000 -0.0000 1.0000 0.0554 -0.0000 0 0 0 -0.9570 0.0062 0 0 -0.0063 1.0200
tau = 14.4000 deg = 25.82 0.2846 0.9510 -0.0146 0.0075 1.0000 0.3336 0.0146 -0.0075 0.0583 0.1160 -0.7353 -0.0822 0.0667 0.0042 -0.0188 0.6967	tau = 14.4000 theta = 26.2755 0.2263 1.0068 0.0000 0 1.0000 0.2264 0 0 0 0 -0.7769 0.0039 0 0 -0.0054 1.0323
tau = 28.8000 deg = 25.82 0.6964 0.9572 -0.0064 0.0125 1.0000 0.7392 0.0064 -0.0125 0.0405 0.0444 -0.3292 -0.0342 0.0465 0.0333 -0.0346 0.4431	tau = 28.8000 theta = 26.2755 0.6175 1.0004 0.0000 0.0000 1.0000 0.6186 0 0 0 0 -0.3821 0.0017 0 0 -0.0028 0.9362

Figure 3: Comparison of Mueller matrix between numerical calculation and experiments for different τ and scattering angle.